A novel role for the tumor suppressor gene *ITF2* in lung tumorigenesis through the action of Wnt signaling pathway.

Olga Pernía[1,2]*, Ana Sastre-Perona[3]*, Carlos Rodriguez-Antolín[1,2], Alvaro García-Guede[1,2], María Palomares-Bralo[4,5], Rocío Rosas[1,2], Darío Sanchez-Cabrero[2], Carmen Rodriguez[1,2], Rubén Martín-Arenas[4,5], Verónica Pulido[1,2], Javier de Castro[2], Pilar Santisteban[3,6], Olga Vera[1,2]+, Inmaculada Ibáñez de Cáceres[1,2]+

[1]Epigenetics laboratory, INGEMM, Hospital La PAZ. Madrid. Spain
[2]Experimental Therapies and novel biomarkers in cancer IdiPAZ. Madrid. Spain
[3]Instituto de Investigaciones Biomedicas CSIC/UAM. Madrid. Spain
[4]Ciber de Enfermedades Raras (CIBERER). Instituto de Salud Carlos III (ISCIII), Madrid. Spain
[5]Laboratorio de Genómica Estructural y Funcional, INGEMM. IdiPAZ. Madrid Spain
[6] Ciber de Cáncer (CIBERONC) Instituto de Salud Carlos III (ISCIII), Madrid. Spain

*** Both authors contributed equally to this work.**
+ Corresponding authors

Corresponding authors:
Inmaculada Ibañez de Caceres E-mail: inma.ibanezca@salud.madrid.org
Olga Vera Puente E-mail: olga.verapuente@moffitt.org
Cancer Epigenetics Laboratory, INGEMM
Biomarkers and Experimental Therapeutics in Cancer, IdiPAZ
Paseo de la Castellana 261, 28046 Madrid, Spain
Phone +34-91-2071010-248; Fax +34-91-2071010

Running title: *ITF2* restores Wnt signaling sensitizing tumor cells to CDDP

Declaration of interest: All the authors have read the journal's authorship statement and declare no potential conflicts of interest.

Competing interests statement: This study was supported by the Fondo de Investigación Sanitaria-Instituto de Salud Carlos III, PI15/00186 and PI18/00050 and by MINECO, RTC-2016-5314-1 to I.I.C; by the MINECO, SAF2016-75531-R, by the CAM B2017/BMD-3724 and by the AECC GCB14142311CRES to P.S; and the European Regional Development Fund/European Social Fund FIS [FEDER/FSE, Una Manera de Hacer Europa].

SUMMARY

Despite often leading to a platinum resistance, platinum-based chemotherapy continues to be the standard treatment for non-small cell lung cancer (NSCLC) and ovarian cancer. In this study, we used array-CGH and qRT-PCR methodologies to identify and validate cytogenetic alterations that arise after cisplatin treatment in four paired cisplatin-sensitive/resistant cell lines. We report that long-term cell exposure to platinum induces an activation of the Wnt pathway that is concomitant with *ITF2* deletion. Restoration of *ITF2* expression normalizes the Wnt pathway activation and re-sensitize tumor cells to platinum. Our translational approach analyzing a total of 55 lung and ovarian primary tumors and control samples, showed a frequent downregulation of *ITF2* expression. As *ITF2* is a negative regulator of the Wnt/β-catenin pathway activity, we used whole transcriptome sequencing (RNA-seq) and Wnt-pathway analysis in a subgroup of NSCLC patients to identify genes with a potential role in the development of this malignancy. Three exhaustive bioinformatics contrasts found three coding genes (*HOXD9*, *RIOX1* and *CLDN6*) and one long non-coding RNA (*XIST*) with significant expression differences (FDR<0.05). Further functional assays overexpressing *ITF2* in cisplatin-resistant cells suggest the regulation of *HOXD9* by the Wnt pathway and its implication on NSCLC progression.

INTRODUCTION

Although platinum-based chemotherapy still plays an important role in the treatment of many solid tumors, the disease progresses to a platinum-resistant state in a high percentage of the diagnosed cases of Non-small cell lung cancer (NSCLC) and ovarian cancer [1, 2] which are two of the most deadly cancers plaguing our society. The former accounting for more than 80% of primary lung-cancer cases and the latter boasting the highest mortality of the gynecological malignancies worldwide [3]. Cisplatin (CDDP) is a platinum compound widely used in the treatment of solid tumors. It induces apoptosis in cancer cells by binding to the N7 position of the guanines and crosslinking DNA [4, 5]. However, CDDP also leads to cytogenetic alterations, such as deletions or amplifications of genes involved in tumor progression, metastasis and drug response [6], which contributes to the development of CDDP-resistance [7-9].

In this study, we performed high resolution million feature array-Comparative Genomic Hybridization (aCGH) with four NSCLC and ovarian cancer sensitive/resistant paired cell lines previously reported by our group [10] to explore the chromosomic deletions that differ in the resistant subtypes. We found a common deletion that includes the Transcription Factor 4, *TCF4* (hereafter called *ITF2*). *ITF2* is a downstream target gene of the Wnt/β-catenin pathway, negatively regulating its activity [11, 12]. Wnt signaling has been identified as one of the key signaling pathways in cancer, and more recently, also involved in drug resistance of primary tumors such as colon or ovarian cancer [13, 14]. However, its role driving platinum resistance in NSCLC has not been defined yet and very little is also known about how ITF2 is involved in tumorigenesis. Therefore, further study of the role of *ITF2* and the Wnt signaling pathway in tumor response to chemotherapy may provide new ways to fight resistance to this popular treatment.

Here we report the frequent downregulation of *ITF2* in NSCLC patients and in cisplatin-resistant cancer cells. Furthermore, we present the Wnt-signaling pathway as a molecular

mechanism behind the development of resistance through the action of *ITF2* and affecting the expression of specific genes that might be also used as potential therapeutic target.

RESULTS

ITF2 is frequently downregulated by chromosomal deletion after CDDP cell exposure

Our cytogenetic study showed different genomic alterations in the CDDP resistant subtypes, using the sensitive parental cell lines as reference genome. We found two deleted regions shared by both tumor types, in at least three of the four cell lines (H23R, A2780R and OVCAR3R) located on 18q21.2-18q21.31 and 18q21.32, affecting the genes *RAB27B, CCDC68, TCF4, TXNL1, WDR7* and *BOD1P;* and genes *ZNF532*, *SEC11C*, *GRP* respectively. We also observed a common deleted region on 2q22.1 that included the gene *LRP1B* in the NSCLC cell lines and an additional common region only shared by the ovarian cancer cell lines on 9q22.33 that included part of the gene *TMOD* (Supplementary Table 1).

We selected *LRP1B* and *TCF4 (ITF2)* genes that were completely deleted in the same tumor type or in at least three of the four cell lines respectively (Figures 1A and Supplementary 1A). The deletion of *ITF2* in H23R and A2780R cell lines resulted in a significant loss of *ITF2* expression compared to the sensitive subtypes, validating the results obtained in the arrays CGH (Figure 1B). No changes were observed neither in OVCAR3 cells for *ITF2* expression nor in H23 and H460 cells for *LRPB1* (Figure 1B and Supplementary Figure 1B).

Wnt canonical signaling pathway is increased in CDDP resistant cells with ITF2 deletions

Due to the association of *ITF2* with the Wnt/B-catenin/TCF pathway, we studied the transcriptional activity of the Wnt pathway in H23S/R and A2780S/R cells, in which the Cisplatin-resistant phenotypes harbors the *ITF2* deletion. We transfected cells with the Wnt reporters (Super8xTop-Fop vectors) and induced the B-catenin/TCF4 activity either by LiCl

treatment, which inhibits GSK3-b, or by co-transfection with the constitutively stable B-catenin-S33Y mutant. We observed higher luciferase activity in A2780R cells compared with the parental sensitive ones, indicating an increased transcriptional activity of B-catenin/TCF in response to both pharmacological and functional activation of the pathway (Figure 2A). This effect was not observed in H23R cells (Figure 2B). We also observed an increase in the gene expression levels of *DKK1* and more slightly in *Cyclin D1*, in A2780 cells two of the four analyzed downstream effectors genes of this pathway (Figure 2C).

Restoration of ITF2 increases the sensitivity to CDDP by decreasing β-catenin/TCF transcriptional activity

To test the role of *ITF2* in cisplatin resistance, we transiently overexpressed *ITF2* cDNA in A2780 cells, in which our previous results confirmed the ability to evaluate changes in the transcriptional activity of the Wnt pathway. Overexpression of ITF2 in A2780R resulted in a significant increase in sensitivity to cisplatin from the dose of 0,5ug/ml ($p<0.01$), showing an intermediate phenotype between the resistant and sensitive subtypes (Figure 3A). In addition, *ITF2* restoration induced a dramatic decrease in cell viability ($p<0.05$) 24 hours after transfection compared with the parental resistant cells transfected with the empty vector (Figure 3B). *ITF2* overexpression at 24 and 72 hours after transfection was confirmed by qRT-PCR (Figure 3C). Moreover, *ITF2* overexpression recovered the levels of B-catenin/TCF transcriptional activity observed in sensitive cells (Figure 3D). In fact, the expression of downstream target *DKK1* was restored from 24h and maintained 72h after *ITF2* overexpression (R-*ITF2*), similar results were also observed at 72h for *Cyclin D1.* (Figure 3E).

The expression of ITF2 is frequently downregulated in NSCLC and ovarian tumor samples

To validate our *in vitro* results we determined the clinical implication of *ITF2* and *DKK1* expression in NSCLC and ovarian cancer patients. The relative expression of both genes

was measured in two cohorts of fresh frozen tumor samples (T) and adjacent tissue (ATT) from NSCLC (Table 1) and ovarian cancer patients (Supplementary Table 2).

We observed that *ITF2* expression is frequently downregulated in NSCLC and ovarian tumor samples (Figure 4) validating our *in vitro* data. Fifteen out of 25 tumor samples of NSCLC patients had lower expression of *ITF2* compared to the normal lungs mean (NLM) (Figure 4A). Furthermore, as reported in our experimental data, we observed the opposite expression profile between *ITF2* and *DKK1* in 60% of NSCLC samples. However, this situation was found only in approximately 10% (1 out of 9) of the ovarian cancer samples (Figure 4B). We did not observe differences between ATT and normal lung samples (LC) for *ITF2* (p=0.177) and *DKK1* (p=0.693) in the NSCLC cohort (Figure 4A).

The Kaplan Meier curves, analyzing the overall survival (OS) according to the median of *ITF2* and *DKK1* expressions, showed that NSCLC patients with high *ITF2* expression tend to have better overall survival, p=0.1 (Figure 4C). No differences in survival were observed for *DKK1* expression p=0.6 (Supplementary Figure 2A). These results were statistically confirmed in 1 926 lung cancer patients by using the Kaplan Meier plotter online tool, noticing that those patients with high expression of *ITF2* (Supplementary Figure 2B) and low expression of *DKK1* (Supplementary Figure 2C) had a significantly better overall survival rate (p=0.016 and p<0.001, respectively).

Identification of candidate genes involved in the Wnt signaling pathway through the analysis of RNA-seq in NSCLC patients

To further explore the role of the Wnt-signaling pathway in lung cancer tumorigenesis, we performed a whole transcriptome analysis performing RNA-seq on 14 samples including nine NSCLC samples, six of them with an inverse expression profile between *ITF2* and *DKK1* (Pat3, Pat6, Pat10, Pat22, Pat25 and Pat26) and three with the same expression profile (Pat8, Pat16 and Pat18). Three ATT (Pat9, Pat21 and Pat25) and two normal lung

samples (LC1 and LC2), were considered as controls for comparisons. *ITF2* was mainly downregulated in NSCLC patients, while *DKK1* showed a more heterogeneous expression pattern. Therefore, we considered *DKK1* as the best parameter to decide the bioinformatics analysis of the RNA-seq. This analysis focused on three main contrasts: contrast A, differential gene expression analysis between tumors and controls, contrast B, comparison between tumors with high and low expression of *DKK1*, and contrast C comparison of the tumor samples with high expression of *DKK1* with the controls (Supplementary Figure 3). We selected those genes that showed significant expression differences (FDR<0.05) in at least two of the three contrasts, prioritizing contrast B (Supplementary Figure 3 and Supplementay Table 3). The bioinformatics analysis also focused in all annotated genes related to the Wnt-pathway.

We analyzed the expression of 9 candidates, but only four of them were detected by qPCR-PCR. Validation of RNA-sequencing results was performed in three coding genes (*HOXD9*, *RIOX1* and *CLDN6*) and one long non-coding RNA (*XIST*). An accurately correlation with the RNA-sequencing data was found for *HOXD9, CLDN6* and *XIST* genes (r=0.83, r=0.97 and r=0.97, respectively) (Figure 5A-C), while for *RIOX1* the correlation coefficient was less marked, probably because of the sample size (r=0.58) (Figure 5D). From all four candidates, only *HOXD9* and *RIOX1* expression showed correlation with *ITF2* expression, (Pearson=-0.24 and Pearson=0.68, respectively) (Figure 5E and 5F). No correlation was found for *XIST* or *CLDN6* (Supplementary Figure 4).

In order to gain insight into the role of *ITF2* regulating the expression of the selected candidates in NSCLC, we overexpressed *ITF2* in H23 lung cancer cells. Transfection efficiency was confirmed by qRT-PCR at 24 and 72 hours after transfection (Figure 6A). As expected from the primary tumors results, the overexpression of *ITF2* induced a significant decrease of *HOXD9* (p=0.04) and an increase of *RIOX1* expressions reaching the levels of the sensitive cells 72 hours after transfection (Figure 6B). Having identified *HOXD9* and *RIOX1* as potential Wnt pathway candidate genes regulated by *ITF2*, we studied their clinical translational application in the cohort of NSCLC patients used for the RNA-seq analysis.

A negative correlation for *HOXD9* and a positive correlation for *RIOX1* was found in terms of patients overall survival (Figure 6C and 6D). In addition, the survival analysis performed by the Kaplan Meier method after stratifying patients according to the median of both genes expression showed that patients with lower expression of *HOXD9* present a significant better overall survival rate (p=0.046), whereas patients with low *RIOX1* expression tend to live less, although no statistical significance was found in this case (Figure 6E and 6F).

DISCUSSION

Wnt signaling has been recently reported to be involved in driving platinum resistance of several tumor types [13, 15]. However, the molecular mechanisms implicated are not clear, specially in NSCLC. In the present work, we have studied the involvement of the Wnt signaling pathway in tumorigenesis through a combined experimental approach by using both CGH arrays and RNA-sequencing. We have found that long term exposure to platinum induces a frequent deletion of *ITF2* that is involved at least in part in the activation of the Wnt pathway.

We firstly identified a common deletion in H23, OVCAR3 and A2780 cells, induced by cisplatin treatment in chromosome 18, including two completely deleted genes, *LRP1B* and *ITF2.* A similar deletion was identified in a previous study where they analysed the cisplatin response in ovarian cancer samples, supporting our results [16]. There is however, another study analyzing the cytogenetic alterations of CDDP-resistant A2780R cells, which shows different genomic alterations. This was probably due to the specificity of the CGH-array used and the experimental design that included less representative number of probes and was performed in only one cell line [8]. We were not able to validate the *LRP1B* expression changes by using an alternative technique, situation that has been previously reported [17]. In our case, it could be due to the mosaicism observed in this region that occurs in less than 20% of the resistant cells. The level of mosaicism that can be detected is dependent on the sensitivity and spatial resolution of the clones and rearrangements present [18].

Nevertheless, *LRP1B* could still play a role in tumor progression as several studies link its downregulation through deletion and carcinogenesis [19-21]. *ITF2* expression changes were confirmed in H23R and A2780R but not in OVCAR3R cells, also probably due to the level of mosaicism (36%) observed in these cells. Our results indicate that low levels of mosaicisms would make the validations of expression changes by another quantitative technique difficult, probably because the alteration at expression levels are not significant enough to be detected.

The fact that *ITF2* is deleted and downregulated after platinum treatment, provides us with a new insight regarding its importance in resistance to platinum chemotherapy in lung and ovarian cancer. Supporting our results a previous study using targeted sequencing in a PDX-based modeling of breast cancer chemoresistance, identified a genomic variant of ITF2 that depicted a link between its altered expression and breast cancer chemoresistance, although no detailed mechanism was provided to connect ITF2 function to chemoresistance [22].

ITF2 is a transcription factor belonging to the basic Helix Loop Helix (bHLH) family, which can act as a transcriptional activator or repressor [23, 24] but its regulation still is unknown. It is important to distinguish *ITF2*, whose real name is TCF4, from the T-Cell Factor 4 (TCF7L2), also known as *TCF4,* which is the bcatenin transcriptional partner [25]. In fact, *ITF2* expression is induced by the B-catenin/TCF complex, but at the same time, it acts as a repressor of this complex by interfering with the binding of B-catenin to TCF4. This causes a decreases in the expression of Wnt target genes, leading to the repression of cell proliferation [12]. Consistent with these studies, we have observed that the resistant A2780 cells have an increased activity of the B-catenin/TCF transcription, which is concomitant with the increased expression of the downstream effector gene DKK1, probably due to the absence of ITF2. In contrast, we did not observe differences in H23 cells, which could be explained by previous observations [26], confirming that H23 has a high basal activity in the Wnt signaling pathway and therefore exogenous activation may not show a difference. Moreover, we have observed that the overexpression of *ITF2* in A2780R cells leads to a

decrease in cell viability, rescuing the sensitive phenotype maybe through the inhibition of the excessive proliferation and the activity levels of the B-catenin/TCF transcription. In fact, our results indicate that resistant cells respond better to the activation of the Wnt pathway, an effect that is restored after the re-expression of *ITF2*. Therefore, the Wnt signaling pathway plays an important role in the resistance to cisplatin through *ITF2* in cancer cell lines.

Our translational analysis, based on the expression levels of *ITF2* and *DKK1* genes in two different cohorts of patients was aimed to elucidate the role of this pathway in tumor progression and chemotherapy response. *ITF2* expression was frequently downregulated in NSCLC and ovarian tumor samples, validating our *in vitro* data. The expression levels of *DKK1*, however, showed a more heterogeneous pattern in the NSCLC tumor samples, while no differences were observed in the ovarian tumors, suggesting an aberrant activation of the Wnt signaling pathway in lung cancer. In fact, our *in silico* analysis of 1 926 NSCLC patients indicates a significant increased overall survival associated with high expression levels of *ITF2* and low expression of *DKK1.* The same findings without statistical significance were observed from our “in house” cohorts, probably due to the sample size. However, one of the strengths of our cohort is that is comprised by fresh frozen samples, enabling us to perform high quality RNA-sequencing in a group of NSCLC patients, in order to determine the involvement of the Wnt-pathway components in lung cancer development. The differential expression of *DKK1* within the tumor samples allowed us to perform three different bioinformatics contrasts in order to explore all the possibilities regarding tumor development and the Wnt signaling pathway. Contrast A aimed to identify genes with a possible involvement in lung cancer development by comparing differential expression in tumors versus control samples. Contrast B was made to identify alterations in the Wnt pathway in NSCLC tumors and those that could be used as potential therapeutic targets. Finally, contrast C was able to identify genes regulated by the Wnt pathway and others involved in NSCLC development. Using this approach we were able to identify coding genes, non-coding genes and transcripts that had not been functionally characterized previously [27,

28]. Indeed, in this study we have identified three coding genes, *HOXD9*, *CLDN6* and *RIOX1*, and one non-coding gene, *XIST*, which could be involved in NSCLC progression through the Wnt signaling pathway. Our data was validated by two alternative methodologies, both showing strong positive correlations of three of the candidates *HOXD9*, *CLDN6* and *XIST* and a slightly weaker correlation for *RIOX1.*

HOXD9 and *CLDN6* were significantly downregulated in tumors with high expression levels of *DKK1* and upregulated in tumors compared with controls, indicating that these genes could be involved in tumor progression through an aberrant activation of the Wnt signaling pathway. In the case of *HOXD9*, the tumor samples had higher expression levels than the controls, as it has been previously reported [29]. We also observed a negative correlation of *HOXD9* and *ITF2* expression levels. In addition, patients with lower levels of *HOXD9* had better overall survival than those with upregulated expression of this gene. These results are consistent with previous studies linking a high expression of *HOXD9* with glioblastoma and hepatocarcinoma [30, 31]. Our functional analysis showed that *ITF2* overexpression in lung cancer cells H23R decreased the expression of *HOXD9*, while we expected a recovery of its expression to the sensitive subtype levels. Therefore we believe that an alternative regulatory mechanism affected by *ITF2* is modulating the expression of *HOXD9*. Reinforcing this hypothesis it has been shown that *HOXD9* expression is also regulated by epigenetic mechanisms such as the long non-coding RNA *HOTAIR* [32, 33], which has been linked with cisplatin-resistance [34]. Although *CLDND6* has been previously associated with carcinogenesis of different tumor types [35, 36], we did not find any correlation with *ITF2* expression levels.

The coding gene *RIOX1* and the non-coding RNA *XIST*, showed an inhibition of their expression in tumor samples with high levels of *DKK1* and in controls. Two different bioinformatic contrasts imply both genes in tumor progression through their regulation by the Wnt signaling pathway. Although an upregulation of *XIST*, which is involved in X-chromosome inactivation [37], has been shown to be involved in tumor development through the Wnt pathway [38], our results do not show a clear correlation with *ITF2* expression or a

relationship with clinical features of NSCLC patients. Conversely, *RIOX1* showed increased expression levels in the tumor samples and a positive correlation with *ITF2* expressio*n*. In addition, patients with higher levels of *RIOX1* tended to have better overall survival than the patients with lower expression levels. Moreover, overexpression of *ITF2* in the H23 lung cancer resistant cells restored the expression level of *RIOX1* to that of the sensitive subtype. Although little is known about *RIOX1*, it has recently been shown to be involved in renal and colorectal carcinogenesis [39, 40]. These results envision these two candidates, who undoubtedly play a role in tumorigenesis, as potential therapeutic targets. In fact, it is becoming clear in the field that a gene can exhibit a double function in cancer, being involved in both tumor development as well as in the response to an antitumor drug, such as *MGMT, IGFBP-3, MAFG* genes or even miRNAs like miR7 [10, 41-44]

In essence, we have identified *ITF2* as a frequently downregulated gene in cisplatin-resistant cancer cells as well as in NSCLC and ovarian cancer patients. Moreover, we define the activation of the Wnt-signaling pathway as a molecular mechanism behind the development of cisplatin resistance in cancer cells through the action of *ITF2,* providing novel insights into the molecular biology and the cellular mechanisms involved in the acquired resistance to the most widely-used chemotherapy agent, cisplatin. Additionally we have suggested two potential therapeutic targets for further study, *ITF2* and *HOXD9.*

MATERIALS AND METHODS

Cell culture and cell-viability assays

The NSCLC and ovarian cancer cell lines H23, H460, OVCAR3 and A2780 were purchased from the ATCC (Manassas, Virginia, USA) and ECACC (Sigma-Aldrich, Madrid, Spain) and cultured as recommended. Their CDDP-resistant variants H23R, H460R, OVCAR3R and A2780R were previously established in our laboratory [10, 45]. Cisplatin (Farma Ferrer, Barcelona, Spain) was used for CDDP-viability assays. Cells were seeded in 24-well dishes at 40,000 cells/well, treated with increasing doses of CDDP (0, 0.5, 1, 1.5, 2 and 3μg/ml) for

an additional 72 or 48 hours and stained as described [46]. Cell viability comparing sensitive vs. resistant cell lines was estimated relative to the density recorded over the same experimental group without drug exposure at same period of time. Cell authentication is included in Supplementary Table 4.

Clinical sample and data collection

We selected a representative number of fresh frozen surgical specimens from University Hospital La Paz (HULP)-Hospital Biobank, totaling 25 NSCLC and 10 ovarian cancer samples, belonging to previously reported cohorts of patients [10]. Ten adjacent normal tissue (ATT) from NSCLC patients, two additional lung tissue samples of non-neoplastic origin from autopsies and ten further normal ovarian samples obtained from sex reassignment surgery or tubal ligation were used as negative controls (NC). All tumor patients had both a perioperative PET-CT scan showing localized disease and a pathological confirmation of stages after having undergone a complete resection for a histologically confirmed tumor. The samples were processed following the standard operating procedures with the appropriate approval of the Human Research Ethics Committee at IdiPAZ, including informed consent within the context of research. Clinical follow-up was conducted according to the criteria of the medical oncology division, pathological and therapeutic data were recorded by an independent observer and a blind statistical analysis was performed on these data.

DNA extraction and array of Comparative Genome Hybridization

DNA from cell lines was isolated as previously described[47] and used to analyze copy number variations by the Array-CGH SurePrint G3 Human CGH Microarray 1x1M (Agilent, Santa Clara, California, USA). Array experiments were performed as recommended by the manufacturer, deeply described in the GEO repository number GSE129692. The Aberration Detection Method 2 (ADM-2) quality weighted interval score algorithm identifies aberrant intervals in samples that have consistently high or low log ratios based on their statistical

score. The score represents the deviation of the weighted average of the normalized log ratios from its expected value of zero calculated with Derivative Log2 Ratio Standard Deviation algorithm. A Fuzzy Zero algorithm is applied to incorporate quality information about each probe measurement. Our threshold settings for the CGH analytics software to make a positive call were 6.0 for sensitivity, 0.45 for minimum absolute average log ratio per region, and 5 consecutive probes with the same polarity were required for the minimum number of probes per region.

RNA extraction, RT-PCR, qRT-PCR

Total RNA from human cancer cell lines and surgical samples was isolated, reverse transcribed and quantitative RT-PCR analysis was performed as previously described[10]. For RT-PCR, 2 µl of the RT product (diluted 1:5) was used for semi-quantitative PCR or qPCR reactions with Promega PCR Mix (Promega, Madison, Wisconsin, USA) and SYBR Green PCR Mix (Applied Biosystems, Waltham, Massachusetts, USA), respectively. RT-PCR was performed under the following conditions: (a) 1 cycle of 95ºC for 2 min; (b) 30–40 cycles of 95ºC for 1 min, 56°C–60ºC for 1 min, 72ºC for 1 min; (c) an extension of 5 min at 72ºC. qRT-PCR absolute quantification was calculated according to the $2^{-\Delta Ct}$ method using GAPDH as endogenous control, whereas relative quantification was calculated with the $2^{-\Delta\Delta Ct}$ using *GAPDH* as endogenous control and the sensitive-parental cell line as a calibrator. Samples were analyzed in triplicate using the HT7900 Real-Time PCR system (Applied Biosystems, USA). Primers and probes for qRT-PCR expression analysis were purchased from Applied Biosystems (*TCF4*: Hs00162613_m1; *LRP1B*: Hs01069120_m1; *DKK1*: Hs00183740_m1; *GADPH*: Hs03929097_g1). Primers for RT-PCR of *Cyclin D1*, *DKK1*, *LEF1*, *TCF3* genes were kindly donated by Dr. Pilar Santisteban (IIBm, Madrid, Spain). Primers for *HOXD9*, *CLDN6*, *XIST* and *RIOX1* were designed, when possible, to analyze the specific transcript that significantly showed changes in the RNA-seq; all primers and specific amplification conditions are listed in Supplementary Table 5.

NGS (RNA-seq) and Wnt signaling pathways analysis

Total RNA from nine tumor tissues, three lung adjacent normal tissue (ATT) from NSCLC samples and two tissue samples of non-neoplastic origin from autopsies were sent to Sistemas Genómicos Company (Valencia, Spain) for RNA-sequencing. Library samples were prepared and sequenced as recommended by the manufacturer (Illumina, San Diego, California, USA) deeply described in the GEO repository number GSE127559. The bioinformatic analysis was performed in the HULP. Reads were analyzed to quantify genes and isoforms through the RSEM-v1.2.3 methodology (RNA-seq by Expectation Maximization)[48] and using the hg19 versions as reference for annotation. The differential expression was carried out with edgeR, which can estimate the common and individual dispersion (CMN and TGW, respectively) to obtain the variability of the data[49]. p-values and FDR statistical analysis were performed by Cmn and Twg models and the statistical cut-off point was set as FDR<0.05. Normalization was performed by the TMM method (Trimmed mean of M-values)[50]. The bioinformatics analysis also included an efficiency analysis for every sample, considering the total efficiency as the percentage of reads annotated belonging to a transcript regarding the total fragments initially read. When using Principal Component Analysis (PCA), no differences were observed between samples from non-neoplastic autopsies and adjacent normal tissue (ATT) from NSCLC patients in terms of transcriptmic profile, therefore both types of samples were considered as a reference group for the differential expression analysis (Supplementary Figure 1). Three different bioinformatics contrasts are described in detail in the Results section.

Transfection assays: top-fop, B-cat and TCF4 Overexpression

A Myc-DDK-tagged ORF clone of *TCF4* and the negative control pCMV6 were used for *in transient* transfection (RC224345; OriGene, Rockville, Maryland, USA) using the previously described methodology[10]. Cells were plated onto 60-mm dishes at 600,000 cells/dish and transfected with a negative control or *TCF4* vectors, using jet-PEI DNA Transfection

Reagent (PolyPlus Transfection, Illkirch, France). For the Wnt reporter assay cells were plated at a concentration of 600,000 cells/well in 6-MW plates. Cells were serum starved overnight and co-transfected with 0.2 µg of either Super8xTopFlash (containing 7 copies of the TCF/LEF binding site) or Super8xFopFlash (containing 6 mutates copies of the TCF/LEF binding sites) expression plasmids, and 0.1µg pRL-TK (Renilla-TK-luciferase vector, Promega, USA) as a control, using Lipofectamine 2000. Cells were subsequently treated with LiCl 10mM or co-transfected with S33Y B-catenin for 48 hours prior to luciferase activities being measured using a Glomax 96 Microplate Luminometer (Turner Biosystems Instrument, Sunnyvale, California, USA). Firefly luciferase activity was calculated as light units normalized with the Renilla activity generated by the pRL-CMV vector. B-catenin/TCF activity was calculated by obtaining the ratio of the Top/Fop promoter activities and expressed in relative terms as the fold change of the untreated cells activation levels (=1).

Statistical analysis

Data were compared using the chi-squared test or Fisher's exact test for qualitative variables, and Student's t test or the Wilcoxon-Mann-Whitney test for quantitative variables. Correlation of quantitative variables was analyzed by Pearson's test. Overall survival was estimated according to the Kaplan-Meier method and compared between groups by means of the Log Rank test. All the p-values were two-sided, and the type I error was set at 5 percent. Statistical analyses were performed using SPSS_20 software (IBM, Armonk, New York, USA).

ACKNOWLEDGEMENTS

The authors thank Hayley Pickett for the English language correction. The authors also acknowledge HULP Biobank for sample processing.

AUTHOR CONTRIBUTIONS

IIC: Conception design and draft

OP, ASP, AGG, MPB, CR, RMA, VP and OVP: development of methodology

OP, ASP, CRA, AGG, RR, DSC, CR, JdC and IIC: acquisition of data

OP, ASP, AGG, RR, DSC, CR, PS, JdC, OVP and IIC: analysis and interpretation of data

CRA and MPB: bioinformatics analysis and interpretation of bioinformatics data

OVP: wrote the manuscript

All authors reviewed and/or revised the manuscript.

IIC and OVP: Approved the final version

IIC and OVP: Agreed to be accountable for all aspects of the work in ensuring that questions related to the accuracy or integrity of any part of the work are appropriately investigated and resolved.

Supplementary information is available online

REFERENCES

1 Lee SY, Jung DK, Choi JE, Jin CC, Hong MJ, Do SK *et al*. PD-L1 polymorphism can predict clinical outcomes of non-small cell lung cancer patients treated with first-line paclitaxel-cisplatin chemotherapy. *Scientific reports* 2016; 6: 25952.

2 French JD, Johnatty SE, Lu Y, Beesley J, Gao B, Kalimutho M *et al*. Germline polymorphisms in an enhancer of PSIP1 are associated with progression-free survival in epithelial ovarian cancer. *Oncotarget* 2016; 7: 6353-6368.

3 Jemal A, Bray F, Center MM, Ferlay J, Ward E, Forman D. Global cancer statistics. *CA: a cancer journal for clinicians* 2011; 61: 69-90.

4 Haslehurst AM, Koti M, Dharsee M, Nuin P, Evans K, Geraci J *et al*. EMT transcription factors snail and slug directly contribute to cisplatin resistance in ovarian cancer. *BMC Cancer* 2012; 12: 91.

5 Karaca B, Atmaca H, Bozkurt E, Kisim A, Uzunoglu S, Karabulut B *et al*. Combination of AT-101/cisplatin overcomes chemoresistance by inducing apoptosis and modulating epigenetics in human ovarian cancer cells. *Mol Biol Rep* 40: 3925-3933.

6 Akervall J, Guo X, Qian CN, Schoumans J, Leeser B, Kort E *et al*. Genetic and expression profiles of squamous cell carcinoma of the head and neck correlate with cisplatin sensitivity and resistance in cell lines and patients. *Clin Cancer Res* 2004; 10: 8204-8213.

7 Hiorns LR, Seckl MJ, Paradinas F, Sharp SY, Skelton LA, Brunstrom G *et al*. A molecular cytogenetic approach to studying platinum resistance. *Journal of inorganic biochemistry* 1999; 77: 95-104.

8 Leyland-Jones B, Kelland LR, Harrap KR, Hiorns LR. Genomic imbalances associated with acquired resistance to platinum analogues. *Am J Pathol* 1999; 155: 77-84.

9 Yasui K, Mihara S, Zhao C, Okamoto H, Saito-Ohara F, Tomida A *et al*. Alteration in copy numbers of genes as a mechanism for acquired drug resistance. *Cancer Res* 2004; 64: 1403-1410.

10 Vera O, Jimenez J, Pernia O, Rodriguez-Antolin C, Rodriguez C, Sanchez Cabo F *et al*. DNA Methylation of miR-7 is a Mechanism Involved in Platinum Response through MAFG Overexpression in Cancer Cells. *Theranostics* 2017; 7: 4118-4134.

11 Kolligs FT, Nieman MT, Winer I, Hu G, Van Mater D, Feng Y *et al*. ITF-2, a downstream target of the Wnt/TCF pathway, is activated in human cancers with beta-catenin defects and promotes neoplastic transformation. *Cancer cell* 2002; 1: 145-155.

12 Shin HW, Choi H, So D, Kim YI, Cho K, Chung HJ *et al*. ITF2 prevents activation of the beta-catenin-TCF4 complex in colon cancer cells and levels decrease with tumor progression. *Gastroenterology* 2014; 147: 430-442 e438.

13 Chikazawa N, Tanaka H, Tasaka T, Nakamura M, Tanaka M, Onishi H *et al*. Inhibition of Wnt signaling pathway decreases chemotherapy-resistant side-population colon cancer cells. *Anticancer Res* 2010; 30: 2041-2048.

14 Nagaraj AB, Joseph P, Kovalenko O, Singh S, Armstrong A, Redline R *et al*. Critical role of Wnt/beta-catenin signaling in driving epithelial ovarian cancer platinum resistance. *Oncotarget* 2015; 6: 23720-23734.

15 Zhang Q, Meng XK, Wang WX, Zhang RM, Zhang T, Ren JJ. The Wnt/beta-catenin signaling pathway mechanism for pancreatic cancer chemoresistance in a three-dimensional cancer microenvironment. *Am J Transl Res* 2016; 8: 4490-4498.

16 Bosquet JG, Marchion DC, Chon H, Lancaster JM, Chanock S. Analysis of chemotherapeutic response in ovarian cancers using publicly available high-throughput data. *Cancer Res* 2014; 74: 3902-3912.

17 Kohno T, Otsuka A, Girard L, Sato M, Iwakawa R, Ogiwara H *et al*. A catalog of genes homozygously deleted in human lung cancer and the candidacy of PTPRD as a tumor suppressor gene. *Genes, chromosomes & cancer* 2010; 49: 342-352.

18 Cho EK. Array-based Comparative Genomic Hybridization and Its Application to Cancer Genomes and Human Genetics. *J Lung Cancer* 2011; 10: 77-86.

19 Brown J, Bothma H, Veale R, Willem P. Genomic imbalances in esophageal carcinoma cell lines involve Wnt pathway genes. *World journal of gastroenterology* 2011; 17: 2909-2923.

20 Ni S, Hu J, Duan Y, Shi S, Li R, Wu H *et al*. Down expression of LRP1B promotes cell migration via RhoA/Cdc42 pathway and actin cytoskeleton remodeling in renal cell cancer. *Cancer science* 2013; 104: 817-825.

21 Liu CX, Musco S, Lisitsina NM, Forgacs E, Minna JD, Lisitsyn NA. LRP-DIT, a putative endocytic receptor gene, is frequently inactivated in non-small cell lung cancer cell lines. *Cancer Res* 2000; 60: 1961-1967.

22 Ruiz de Garibay G, Mateo F, Stradella A, Valdes-Mas R, Palomero L, Serra-Musach J *et al*. Tumor xenograft modeling identifies an association between TCF4 loss and breast cancer chemoresistance. *Dis Model Mech* 2018; 11.

23 Murre C. Helix-loop-helix proteins and lymphocyte development. *Nature immunology* 2005; 6: 1079-1086.

24 Sepp M, Kannike K, Eesmaa A, Urb M, Timmusk T. Functional diversity of human basic helix-loop-helix transcription factor TCF4 isoforms generated by alternative 5' exon usage and splicing. *PLoS One* 2011; 6: e22138.

25 Navarrete K, Pedroso I, De Jong S, Stefansson H, Steinberg S, Stefansson K *et al*. TCF4 (e2-2; ITF2): a schizophrenia-associated gene with pleiotropic effects on human disease. *American journal of medical genetics Part B, Neuropsychiatric genetics : the official publication of the International Society of Psychiatric Genetics* 2013; 162B: 1-16.

26 Akiri G, Cherian MM, Vijayakumar S, Liu G, Bafico A, Aaronson SA. Wnt pathway aberrations including autocrine Wnt activation occur at high frequency in human non-small-cell lung carcinoma. *Oncogene* 2009; 28: 2163-2172.

27 Wang Z, Gerstein M, Snyder M. RNA-Seq: a revolutionary tool for transcriptomics. *Nat Rev Genet* 2009; 10: 57-63.

28 Katz Y, Wang ET, Airoldi EM, Burge CB. Analysis and design of RNA sequencing experiments for identifying isoform regulation. *Nat Methods* 2010; 7: 1009-1015.

29 Plowright L, Harrington KJ, Pandha HS, Morgan R. HOX transcription factors are potential therapeutic targets in non-small-cell lung cancer (targeting HOX genes in lung cancer). *Br J Cancer* 2009; 100: 470-475.

30 Tabuse M, Ohta S, Ohashi Y, Fukaya R, Misawa A, Yoshida K *et al*. Functional analysis of HOXD9 in human gliomas and glioma cancer stem cells. *Mol Cancer* 2011; 10: 60.

31 Lv X, Li L, Lv L, Qu X, Jin S, Li K *et al*. HOXD9 promotes epithelial-mesenchymal transition and cancer metastasis by ZEB1 regulation in hepatocellular carcinoma. *J Exp Clin Cancer Res* 2015; 34: 133.

32 Rinn JL, Kertesz M, Wang JK, Squazzo SL, Xu X, Brugmann SA *et al*. Functional demarcation of active and silent chromatin domains in human HOX loci by noncoding RNAs. *Cell* 2007; 129: 1311-1323.

33 Woo CJ, Kingston RE. HOTAIR lifts noncoding RNAs to new levels. *Cell* 2007; 129: 1257-1259.

34 Liu Z, Sun M, Lu K, Liu J, Zhang M, Wu W *et al*. The long noncoding RNA HOTAIR contributes to cisplatin resistance of human lung adenocarcinoma cells via downregualtion of p21(WAF1/CIP1) expression. *PLoS One* 2013; 8: e77293.

35 Ikenouchi J, Matsuda M, Furuse M, Tsukita S. Regulation of tight junctions during the epithelium-mesenchyme transition: direct repression of the gene expression of claudins/occludin by Snail. *J Cell Sci* 2003; 116: 1959-1967.

36 Lu Y, Wang L, Li H, Li Y, Ruan Y, Lin D *et al*. SMAD2 Inactivation Inhibits CLDN6 Methylation to Suppress Migration and Invasion of Breast Cancer Cells. *Int J Mol Sci* 2017; 18.

37 Brown SD. XIST and the mapping of the X chromosome inactivation centre. *Bioessays* 1991; 13: 607-612.

38 Sun N, Zhang G, Liu Y. Long non-coding RNA XIST sponges miR-34a to promotes colon cancer progression via Wnt/beta-catenin signaling pathway. *Gene* 2018; 665: 141-148.

39 Pires-Luís AS, Vieira-Coimbra M, Vieira FQ, Costa-Pinheiro P, Silva-Santos R, Dias PC *et al*. Expression of histone methyltransferases as novel biomarkers for renal cell tumor diagnosis and prognostication. *Epigenetics* 2015; 10: 1033-1043.

40 Nishizawa Y, Nishida N, Konno M, Kawamoto K, Asai A, Koseki J *et al*. Clinical Significance of Histone Demethylase NO66 in Invasive Colorectal Cancer. *Ann Surg Oncol* 2017; 24: 841-849.

41 Belhadj S, Moutinho C, Mur P, Setien F, Llinas-Arias P, Perez-Salvia M *et al*. Germline variation in O(6)-methylguanine-DNA methyltransferase (MGMT) as cause of hereditary colorectal cancer. *Cancer Lett* 2019; 447: 86-92.

42 Chen X, Zhang M, Gan H, Wang H, Lee JH, Fang D *et al*. A novel enhancer regulates MGMT expression and promotes temozolomide resistance in glioblastoma. *Nat Commun* 2018; 9: 2949.

43 Cortes-Sempere M, de Miguel MP, Pernia O, Rodriguez C, de Castro Carpeno J, Nistal M *et al*. IGFBP-3 methylation-derived deficiency mediates the resistance to cisplatin through the activation of the IGFIR/Akt pathway in non-small cell lung cancer. *Oncogene* 2013; 32: 1274-1283.

44 Vera-Puente O, Rodriguez-Antolin C, Salgado-Figueroa A, Michalska P, Pernia O, Reid BM *et al*. MAFG is a potential therapeutic target to restore chemosensitivity in cisplatin-resistant cancer cells by increasing reactive oxygen species. *Transl Res* 2018.

45 Ibanez de Caceres I, Cortes-Sempere M, Moratilla C, Machado-Pinilla R, Rodriguez-Fanjul V, Manguan-Garcia C *et al*. IGFBP-3 hypermethylation-derived deficiency mediates cisplatin resistance in non-small-cell lung cancer. *Oncogene* 2010; 29: 1681-1690.

46 Chattopadhyay S, Machado-Pinilla R, Manguan-Garcia C, Belda-Iniesta C, Moratilla C, Cejas P *et al*. MKP1/CL100 controls tumor growth and sensitivity to cisplatin in non-small-cell lung cancer. *Oncogene* 2006; 25: 3335-3345.

47 Ibanez de Caceres I, Dulaimi E, Hoffman AM, Al-Saleem T, Uzzo RG, Cairns P. Identification of novel target genes by an epigenetic reactivation screen of renal cancer. *Cancer Res* 2006; 66: 5021-5028.

48 Li B, Dewey CN. RSEM: accurate transcript quantification from RNA-Seq data with or without a reference genome. *BMC bioinformatics* 2011; 12: 323.

49 Robinson MD, McCarthy DJ, Smyth GK. edgeR: a Bioconductor package for differential expression analysis of digital gene expression data. *Bioinformatics* 2010; 26: 139-140.

50 Robinson MD, Oshlack A. A scaling normalization method for differential expression analysis of RNA-seq data. *Genome biology* 2010; 11: R25.

FIGURE LEGENDS

Figure 1. Identification of a common deletion in chromosome 18 in cisplatin-resistant cancer cell lines. (A) Picture extracted from the Agilent Cytogenomics 3.0.1.1 software showing the *ITF2* deletion in chromosome 18 in H23R, A2780R and OVCAR3R cell lines. (B) Relative mRNA expression levels of *ITF2* measured by qRT-PCR. The results show the mean fold induction compared to the sensitive cells. Gene expression was normalized to *GAPDH*. S: sensitive; R: resistant; Data represent the relative expression levels obtained from the combination of two independent experiments measured in triplicate ± SD.
*** $p < 0.001$; (Students T-test).

Figure 2. Basal status of the Wnt signaling pathway in A2780 and H23 cell lines. (A) Pharmacological activation (left) and functional activation (right) of β-catenin transcriptional activity in A2780 cells. (B) Pharmacological activation of β-catenin transcriptional activity in H23 cells. β-catenin transcriptional activity was measure in A2780 and H23 cells after treatment with LiCl (10mM) 24 hours or transfection of bcat-S33Y, transfecting with Super8xTopFlash (Top) or Super8xFopFlash (Fop). The results show the fold induction of the Top/Fop ratio with respect to untreated cells (=1). Values represent the mean of three independent experiments measured by triplicate ± SD. *** $p < 0.001$; ** $p < 0.01$ (Students T-test). (C) Expression analysis of downstream genes regulated by *ITF2* involved in Wnt signaling pathway in H23S and H23R and A2780S and A2780R. Representative images of *LEF1, Cyclin D1, TCF3, DKK1* and *GAPDH* measured by RT-PCR. Each assay was performed at least three times to confirm the results.

Figure 3. Effect of *ITF2* on cisplatin resistance, cell viability and Wnt pathway. (A) Viability curves of A2780 cell lines transfected with pCMV6 (S-Ø and R-Ø) and with the overexpression vector (R-ITF2). Each experimental group was exposed to 6 different CDDP concentrations for 48 h. Data were normalized to each untreated control, set to 100%. The data represent the mean ± SD of at least three independent experiments performed in quadruplicate at each drug concentration for each cell line analyzed. (B) Viability of A2780 cell lines transfected with pCMV6 (R-Ø) and with the overexpression vectors (R-ITF2). (C) Relative expression levels of *ITF2* measured by quantitative RT-PCR, represented in Log10 scale; In each experimental group, the sensitive cell line transfected with pCMV6 plasmid was used as a calibrator. Each bar represents the combined relative expression of two independent experiments measured in triplicate. (D) β-catenin transcriptional activity was measured in A2780 cells after *ITF2* overexpression and treatment with LiCl (10mM) for 24 hours, transfecting with Super8xTopFlash (Top) or Super8xFopFlash (Fop). The results show the fold induction of the Top/Fop ratio with respect to untreated cells (=1). Values represent the mean of three independent experiments measured by triplicate ± SD. (E) Expression analysis of the downstream genes DKK1 and Cyclin D1 regulated by *ITF2* in A2780 cell line transfected with pCMV6 (S-Ø and R-Ø) and with the overexpression vector (R-ITF2) for 24 and 72 hours. Left, representative images of *DKK1, Cyclin D1* and *GAPDH* measured by RT-PCR. Right, expression levels of *DKK1* and *Cyclin D1* measured by qPCR. Each assay was performed at least three times to confirm the results. *** $p < 0.001$; ** $p < 0.01$ (Students T-test).

Figure 4. Expression profile of *ITF2* and *DKK1* in patients with NSCLC and ovarian cancer. (A-B) Assessment of *ITF2* and *DKK1* expression levels measured by qRT-PCR in 55 fresh samples from non-tumor samples and two cohort NSCLC (A) and ovarian cancer patients(B). For all the analyses, data represents expression levels in 2-ΔΔCt using the mean of normal lungs (NLM) or ovarian (NOM) as calibrator. (C) Survival analysis in 25 NSCLC samples according to the mean of *ITF2* expression. LogRank, Breslow and Tarone-Ware test were used for comparisons and p<.05 was considered as a significant change in OS. NSCLC: non-small cell lung cancer; ATT: adjacent tumor tissue; T: tumor; LC1/LC2: Lung Control; NLM: Normal Lung Mean; NOM: Normal Ovarian Mean.

Figure 5. Expression levels of candidate target genes measured by RNA-seq and qRT-PCR and correlation with *ITF2* expression levels in tumor and non-tumor samples from NSCLC patients. (A-D) correlation between RNA-seq and qRT-PCR expression levels performed in a selection of 14 samples in *HOXD9* (A), *XIST* (B), *CLDN6* (C) and *RIOX1* (D). Bars represent the relative expression of each gene measured by qRT-PCR in triplicate and represented as $2^{-\Delta Ct}$ and lines represent the count per million obtained from the RNA-seq analysis. (E-F) correlation between *ITF2* expression and *HOXD9* (E) and *RIOX1* (F) in the complete cohort of 25 NSCLC patients. Pearson coefficient was used for linear correlation of the quantitative variables

Figure 6. Effect of *ITF2* overexpression over its candidate target genes in vitro and in nine NSCLC patients samples. (A) Validation of the transfection efficiency of *ITF2* at mRNA levels. Relative expression levels of *ITF2* measured by qRT-PCR, in the cell line H23, at 24 and 72 hour after transfection represented in Log10 the 2-ΔΔCt. (B) Relative expression levels of *HOXD9* and *RIOX1* measured by quantitative RT-PCR after *ITF2* overexpression. For both (A) and (B) the sensitive cell line transfected with pCMV6 plasmid was used as a calibrator (S-Ø). H23R cells were transfected with same negative control (R-Ø) or with ITF2 cDNA (R-ITF2). Each bar represents the combined relative expression of two independent experiments measured in triplicate. *** p < 0.001; ** p < 0.01 (Students T-test). (C and D) Analysis of *ITF2* and its candidate target genes in nine NSCLC patients. Correlation between *ITF2* and *HOXD9* (C) expression levels and *ITF2* and *RIOX1* (D) with the overall survival analyzed by RNA-seq. Data represents the quantitative expression levels of the three genes measured by qRT-PCR and represented as 2-ΔΔCt for *ITF2* (referred to the NLM) and 2-ΔCt for *HOXD9* and *RIOX1*. (E) Survival analysis in NSCLC samples according to the mean of HOXD9 and (F) RIOX1 expression levels. LogRank, Breslow and Tarone-Ware test were used for comparisons and p < 0.05 was considered as a significant change in OS.

Table 1. Clinicopathological and experimental data obtained from patients with NSCLC from La Paz University Hospital. Note: OS, Overall Survival; PFS, Progression Free Survival; CDDP: cisplatin; CBDCA: carboplatin; NA: not available.

Patient	Histology	Sex	Stage	Chemotherapy	Relapse	Status	OS (days)	PFS (days)	*TCF4* ($2^{-\Delta Ct}$)	*DKK1* ($2^{-\Delta Ct}$)	*HOXD9* ($2^{-\Delta Ct}$)	*RIOX1* ($2^{-\Delta Ct}$)
Pat1.T	Adenocarcinoma	Female	IA	No	Yes	Alive	2220	1490	0.03364	0.00089	8.2E-05	0.00872
Pat2.T	Adenocarcinoma	Male	NA	No	Yes	Alive	2352	1860	0.01041	0.00003	0.04277	0.01605
Pat3.T	Epidermoid	Male	IB	No	Yes	Exitus	1022	825	0.01012	0.00075	8.2E-06	0.00114
Pat4.T	Adenocarcinoma	Male	IB	No	No	Exitus	3	3	0.00286	0.00006	0.00041	0.00624
Pat5.T	Adenocarcinoma	Male	NA	No	No	Exitus	626	626	0.00365	0.00005	0.00503	0.00932
Pat6.T	Large cell	Male	IIB	No	No	Exitus	62	62	0.01584	0.00119	0.00074	0.00216
Pat7.T	Adenocarcinoma	Male	IIIA	Otro	Yes	Exitus	228	138	0.01278	0.00150	0.00078	0.1207
Pat8.T	Epidermoid	Female	IIIB	CDDP + Others	No	Exitus	109	109	0.00675	0.00026	0.00126	0.00196
Pat9.T	Adenocarcinoma	Female	IIA	CDDP + Others	Yes	Alive	2260	2260	0.01070	0.01826	0.00097	0.04697
Pat10.T	Epidermoid	Male	IB	No	No	Alive	1853	1853	0.01626	0.00162	0.00027	0.00723
Pat11.T	Adenocarcinoma	Male	IA	No	No	Exitus	216	216	0.00456	0.00003	0.0007	0.01399
Pat12.T	Adenocarcinoma	Female	IIIA	CBDCA + Others	Yes	Alive	2192	2192	0.00580	0.00004	0.00146	0.01059
Pat13.T	Epidermoid	Male	IB	CDDP + Others	No	Alive	2341	2341	0.02466	0.00090	0.00013	0.14752
Pat14.T	Epidermoid	Male	IIA	No	ND	Exitus	289	289	0.01179	0.00206	0.00061	0.02547
Pat15.T	Epidermoid	Male	IIA	No	ND	ND	109	109	0.01833	0.01370	0.0042	0.07619
Pat16.T	Adenocarcinoma	Female	IIIA	CDDP + Others	ND	Alive	2228	2228	0.00907	0.00005	0.00191	0.00814
Pat17.T	Adenocarcinoma	Male	IIB	Otro	Yes	Exitus	888	443	0.00704	0.00014	1.6E-05	0.00833
Pat18.T	Epidermoid	Male	IIB	CBDCA + Others	No	Exitus	259	259	0.00563	0.00001		0.01455
Pat19.T	Adenocarcinoma	Female	IB	CDDP + Others	Yes	Exitus	936	428	0.00738	0.00137	0.00014	0.01572
Pat20.T	Epidermoid	Male	IIB	CDDP + Others	Yes	Exitus	1224	637	0.00346	0.00089	0.00264	0.00422
Pat22.T	Adenocarcinoma	Male	IIIA	CDDP + Others	No	ND	421	421	0.00792	0.00279	3.2E-05	0.00509
Pat23.T	Adenocarcinoma	Female	IIB	CDDP + Others	ND	ND	184	184	0.01319	0.00101	6.8E-05	0.0148
Pat24.T	Epidermoid	Male	IIIA	CDDP + Others	ND	ND	542	542	0.03221	0.00214	0.0012	0.01741
Pat25.T	Adenocarcinoma	Male	IIA	CBDCA + Others	No	Alive	1491	1491	0.0368	0.00614	0.00077	0.01088
Pat26.T	Adenocarcinoma	Male	IIA	CDDP + Others	No	Alive	1496	1496			0.00008	0.00872

Figure1

A

H23R

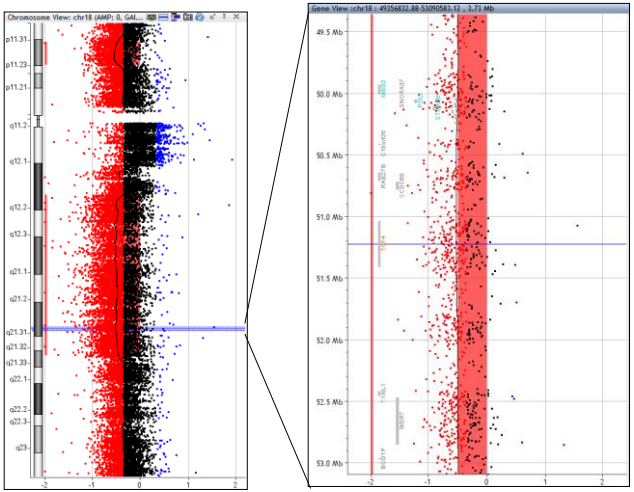

A2780R

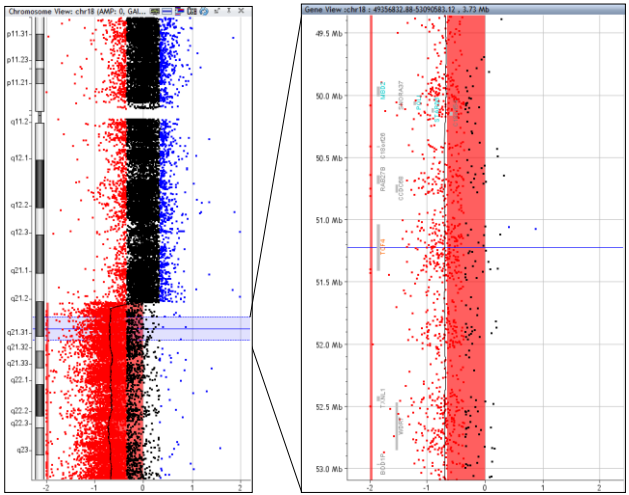

OVCAR3R

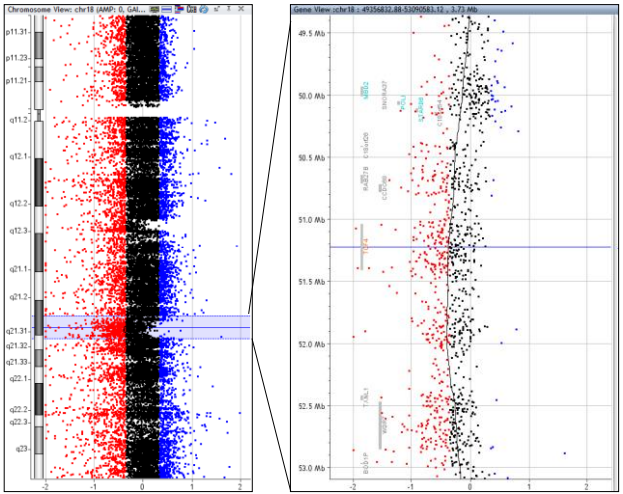

B

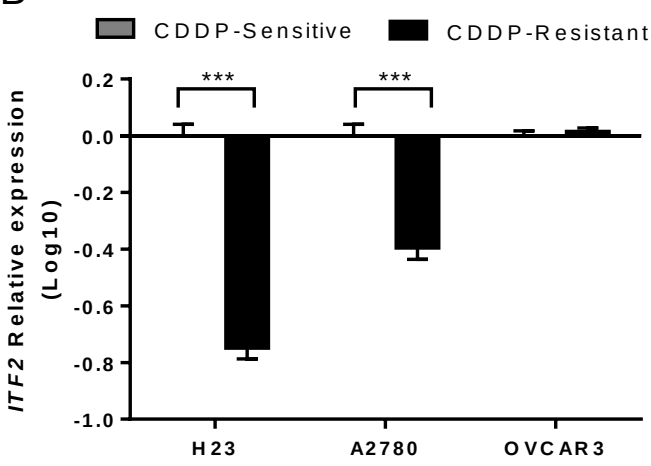

Figure2

A

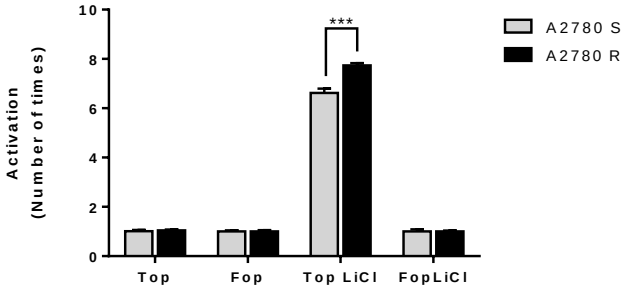
Activation
(Number of times)
10
8
6
4
2
0
***
A2780 S
A2780 R
Top
Fop
Top LiCl
FopLiCl

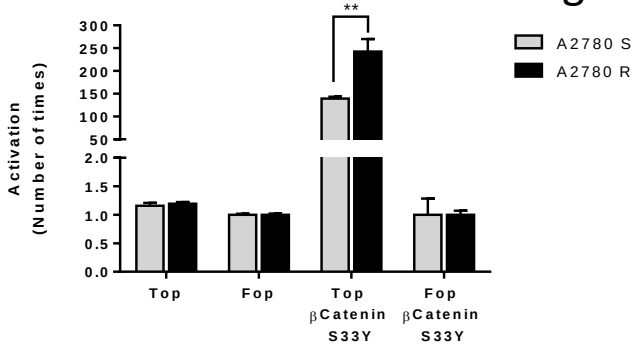
Activation
(Number of times)
300
250
200
150
100
50
2.0
1.5
1.0
0.5
0.0
**
A2780 S
A2780 R
Top
Fop
Top
βCatenin
S33Y
Fop
βCatenin
S33Y

B

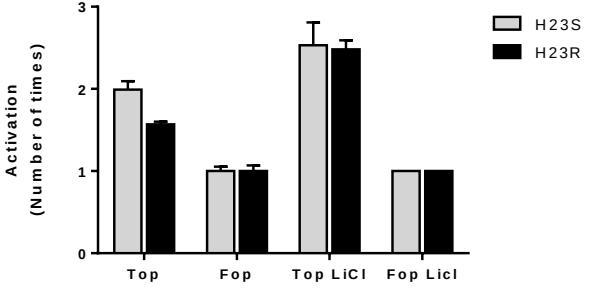
Activation
(Number of times)
3
2
1
0
H23S
H23R
Top
Fop
Top LiCl
Fop Licl

C

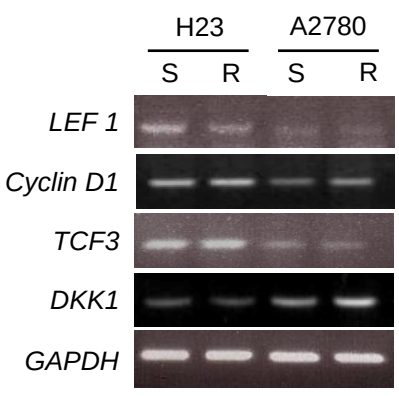
H23
A2780
S
R
S
R
LEF 1
Cyclin D1
TCF3
DKK1
GAPDH

Figure3

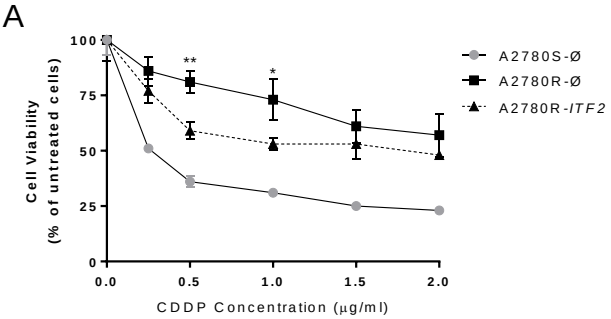
A
Cell Viability
(% of untreated cells)
100
75
50
25
0
0.0
0.5
1.0
1.5
2.0
CDDP Concentration (μg/ml)
**
*
A2780S-Ø
A2780R-Ø
A2780R-ITF2

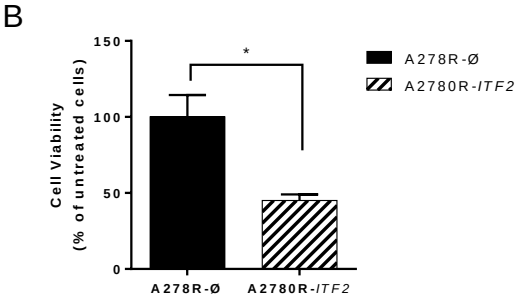
B
Cell Viability
(% of untreated cells)
150
100
50
0
*
A278R-Ø
A2780R-ITF2
A278R-Ø
A2780R-ITF2

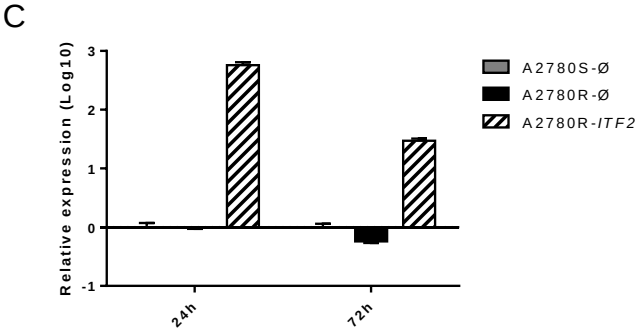
C
Relative expression (Log10)
3
2
1
0
-1
24h
72h
A2780S-Ø
A2780R-Ø
A2780R-ITF2

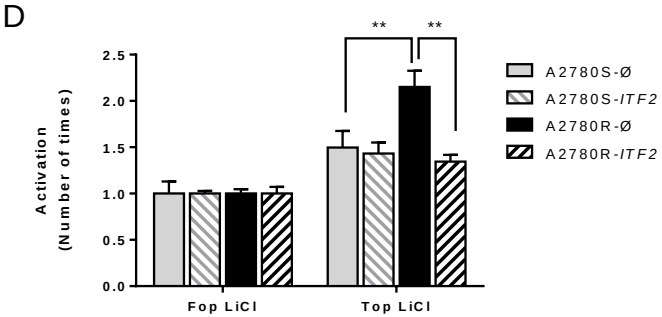
D
Activation
(Number of times)
2.5
2.0
1.5
1.0
0.5
0.0
**
**
Fop LiCl
Top LiCl
A2780S-Ø
A2780S-ITF2
A2780R-Ø
A2780R-ITF2

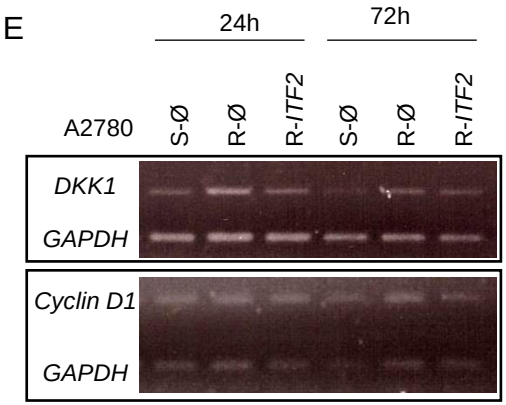
E
24h
72h
A2780
S-Ø
R-Ø
R-ITF2
S-Ø
R-Ø
R-ITF2
DKK1
GAPDH
Cyclin D1
GAPDH

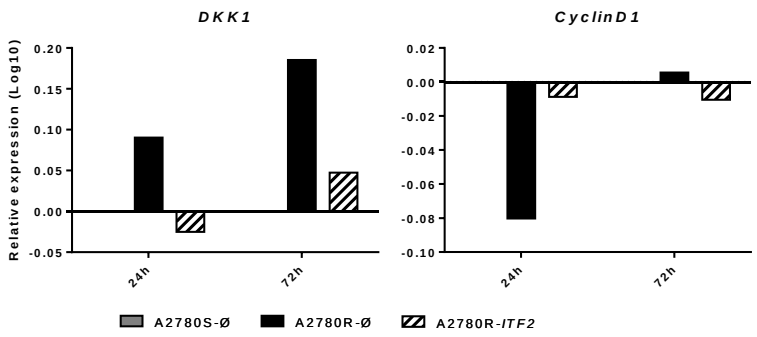
DKK1
CyclinD1
Relative expression (Log10)
0.20
0.15
0.10
0.05
0.00
-0.05
0.02
0.00
-0.02
-0.04
-0.06
-0.08
-0.10
24h
72h
24h
72h
A2780S-Ø
A2780R-Ø
A2780R-ITF2

Figure4

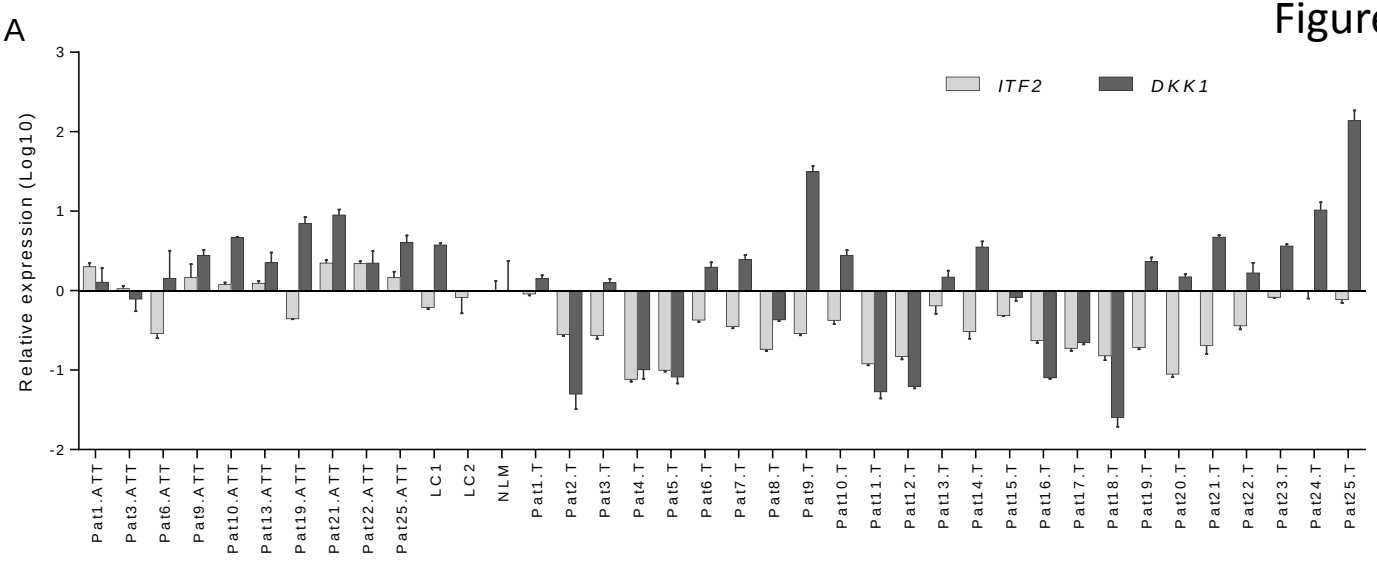
A
ITF2
DKK1
Relative expression (Log10)
3
2
1
0
-1
-2
Pat1.ATT
Pat3.ATT
Pat6.ATT
Pat9.ATT
Pat10.ATT
Pat13.ATT
Pat19.ATT
Pat21.ATT
Pat22.ATT
Pat25.ATT
LC1
LC2
NLM
Pat1.T
Pat2.T
Pat3.T
Pat4.T
Pat5.T
Pat6.T
Pat7.T
Pat8.T
Pat9.T
Pat10.T
Pat11.T
Pat12.T
Pat13.T
Pat14.T
Pat15.T
Pat16.T
Pat17.T
Pat18.T
Pat19.T
Pat20.T
Pat21.T
Pat22.T
Pat23.T
Pat24.T
Pat25.T

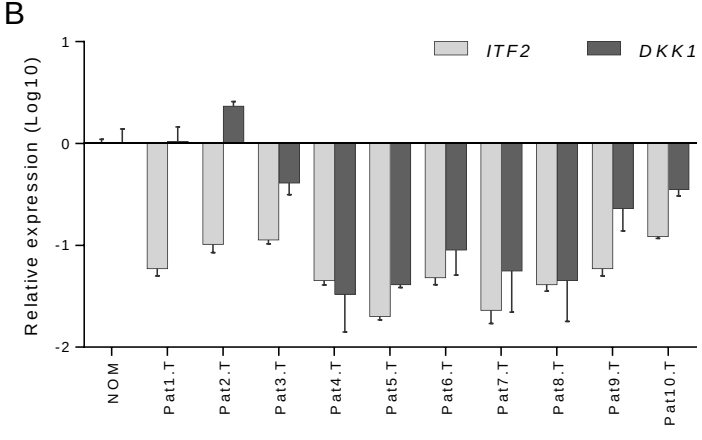
B
ITF2
DKK1
Relative expression (Log10)
1
0
-1
-2
NOM
Pat1.T
Pat2.T
Pat3.T
Pat4.T
Pat5.T
Pat6.T
Pat7.T
Pat8.T
Pat9.T
Pat10.T

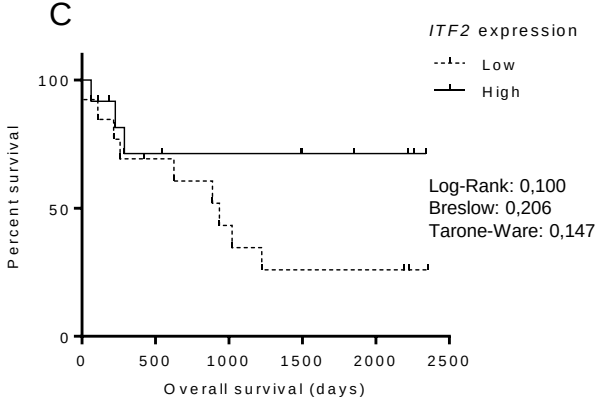
C
ITF2 expression
Low
High
Percent survival
100
50
0
0
500
1000
1500
2000
2500
Overall survival (days)
Log-Rank: 0,100
Breslow: 0,206
Tarone-Ware: 0,147

Figure5

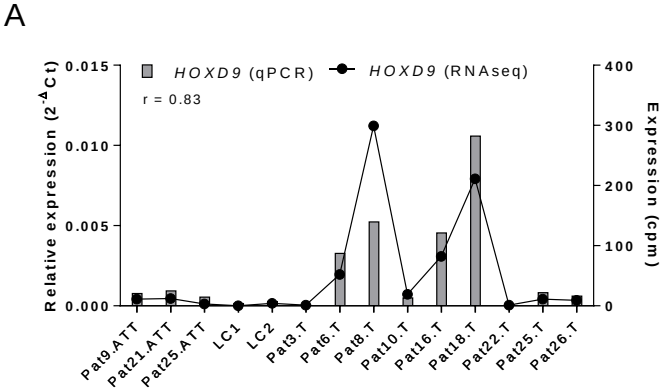
A
HOXD9 (qPCR)
HOXD9 (RNAseq)
r = 0.83
Relative expression (2-ΔCt)
Expression (cpm)
0.015
0.010
0.005
0.000
400
300
200
100
0
Pat9.ATT
Pat21.ATT
Pat25.ATT
LC1
LC2
Pat3.T
Pat6.T
Pat8.T
Pat10.T
Pat16.T
Pat18.T
Pat22.T
Pat25.T
Pat26.T

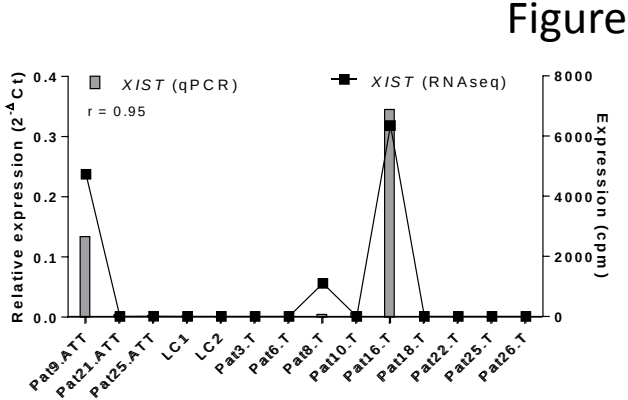
B
XIST (qPCR)
XIST (RNAseq)
r = 0.95
Relative expression (2-ΔCt)
Expression (cpm)
0.4
0.3
0.2
0.1
0.0
8000
6000
4000
2000
0
Pat9.ATT
Pat21.ATT
Pat25.ATT
LC1
LC2
Pat3.T
Pat6.T
Pat8.T
Pat10.T
Pat16.T
Pat18.T
Pat22.T
Pat25.T
Pat26.T

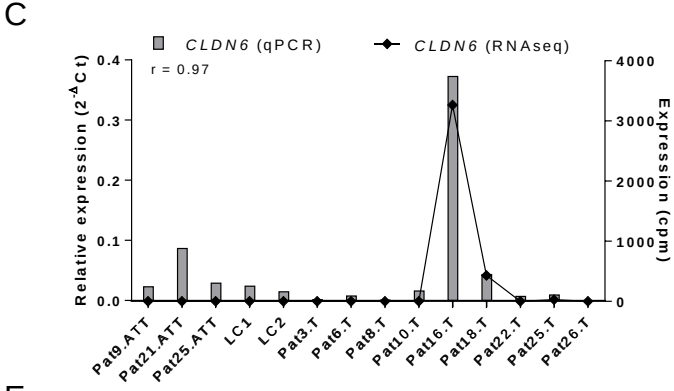
C
CLDN6 (qPCR)
CLDN6 (RNAseq)
r = 0.97
Relative expression (2-ΔCt)
Expression (cpm)
0.4
0.3
0.2
0.1
0.0
4000
3000
2000
1000
0
Pat9.ATT
Pat21.ATT
Pat25.ATT
LC1
LC2
Pat3.T
Pat6.T
Pat8.T
Pat10.T
Pat16.T
Pat18.T
Pat22.T
Pat25.T
Pat26.T

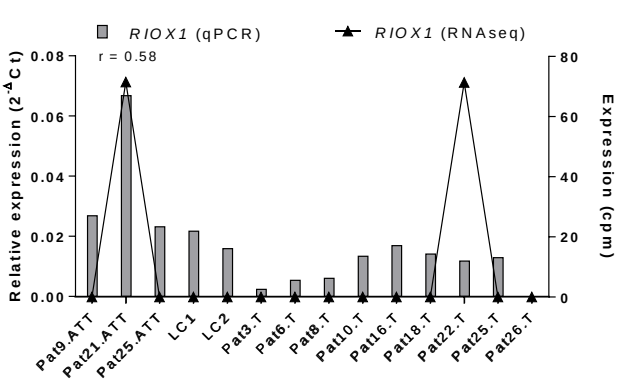
D
RIOX1 (qPCR)
RIOX1 (RNAseq)
r = 0.58
Relative expression (2-ΔCt)
Expression (cpm)
0.08
0.06
0.04
0.02
0.00
80
60
40
20
0
Pat9.ATT
Pat21.ATT
Pat25.ATT
LC1
LC2
Pat3.T
Pat6.T
Pat8.T
Pat10.T
Pat16.T
Pat18.T
Pat22.T
Pat25.T
Pat26.T

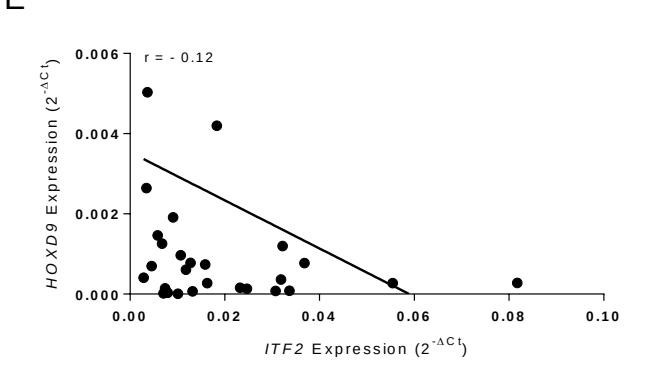
E
r = - 0.12
HOXD9 Expression (2-ΔCt)
ITF2 Expression (2-ΔCt)
0.006
0.004
0.002
0.000
0.00
0.02
0.04
0.06
0.08
0.10

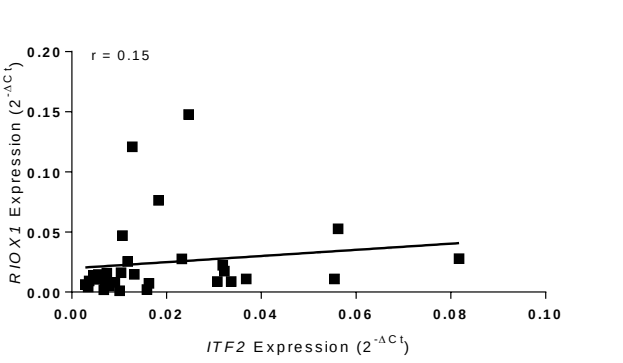
F
r = 0.15
RIOX1 Expression (2-ΔCt)
ITF2 Expression (2-ΔCt)
0.20
0.15
0.10
0.05
0.00
0.00
0.02
0.04
0.06
0.08
0.10

Figure6

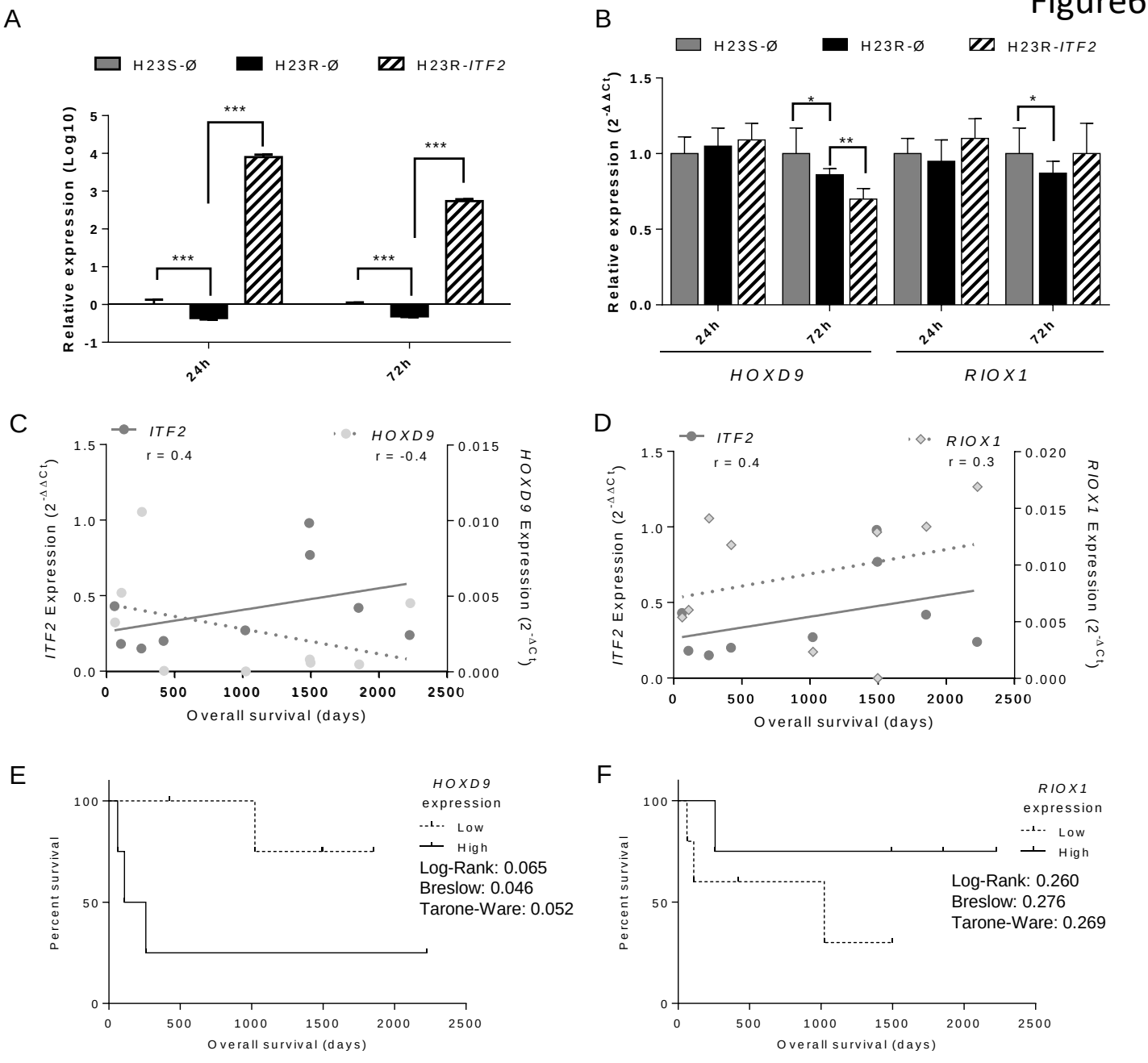
A
H23S-Ø
H23R-Ø
H23R-ITF2
Relative expression (Log10)
***
24h
72h
B
H23S-Ø
H23R-Ø
H23R-ITF2
Relative expression (2^-ΔΔCt)
*
**
24h
72h
HOXD9
RIOX1
C
ITF2
r = 0.4
HOXD9
r = -0.4
ITF2 Expression (2^-ΔΔCt)
HOXD9 Expression (2^-ΔCt)
Overall survival (days)
D
ITF2
r = 0.4
RIOX1
r = 0.3
ITF2 Expression (2^-ΔΔCt)
RIOX1 Expression (2^-ΔCt)
Overall survival (days)
E
HOXD9
expression
Low
High
Log-Rank: 0.065
Breslow: 0.046
Tarone-Ware: 0.052
Percent survival
Overall survival (days)
F
RIOX1
expression
Low
High
Log-Rank: 0.260
Breslow: 0.276
Tarone-Ware: 0.269
Percent survival
Overall survival (days)